CONTRAST MEDIA & MOLECULAR IMAGING

Received: 23 January 2008, Revised: 9 July 2008, Accepted: 11 July 2008, Published online in Wiley InterScience: 29 August 2008

(www.interscience.wiley.com) DOI:10.1002/cmmi.241

Cobalt nanoparticles as a novel magnetic resonance contrast agent—relaxivities at 1.5 and 3 Tesla

Laura M. Parkes[a]*, Richard Hodgson[a], Le T. Lu[b], Le D. Tung[c], Ian Robinson[b], David G. Fernig[d,e] and Nguyen T. K. Thanh[b,d,e]

Two samples of polymer-coated cobalt nanoparticles were synthesized and dispersed in agarose gel and water. The relaxivities r_1 and r_2 of the two samples were obtained at different temperatures (25, 37 and 40°C) and magnetic field strengths (1.5 and 3 T). The average cobalt core diameters of the two samples were 3.3 and 3.9 nm (measured by transmission electron microscopy); the corresponding average total diameters (cobalt core + polymer coating) were 13 and 28 nm (measured by dynamic light scattering). The larger particles had the higher r_1 relaxivity, whilst r_2 was similar for the two samples. There was no significant change in r_1 or r_2 relaxivities with temperature but r_1 at 1.5 T was approximately double the value at 3 T. The highest relaxivities were obtained at 1.5 T with values for r_1 and r_2 of 7.4 and 88 $mM^{-1}s^{-1}$, respectively. These values are similar to those reported for iron oxide with larger core size, suggesting the potential of the cobalt nanoparticles for development and future use as a negative contrast agent.

Keywords: cobalt; nanoparticles; USPIO; MR contrast agents; relaxometry

1. INTRODUCTION

Magnetic nanoparticles offer a unique opportunity for cell tracking *in vivo*. By incorporating magnetic nanoparticles inside cells, their position within the body can be tracked using magnetic resonance imaging (MRI). Currently, iron oxide nanoparticles (ultra-small superparamagnetic iron oxide, USPIOs) are widely used as contrast agents in MRI (1,2). However, iron oxide has a relatively low saturation magnetization, requiring the use of large particles to achieve sufficient magnetic resonance (MR) contrast. On the other hand, transition metals, for example cobalt, have much higher saturation magnetization value [1422 emu/cm^3 for cobalt (3) compared with 395 emu/cm^3 for iron oxide (4) at room temperature]. This means that cobalt nanoparticles may have a larger effect on proton relaxation, giving improved MR contrast and allowing smaller particle cores to be used without compromising sensitivity.

In this paper, the magnetic properties and MR characteristics of cobalt nanoparticles are presented. Two samples with different average particle sizes were synthesized to test the effect of the production process and MR properties. The relaxation rates R_1 and R_2 were measured at a range of concentrations and the relaxivities r_1 and r_2 were calculated. These were measured at three temperatures (25, 37 and 40°C) and two magnetic field strengths (1.5 and 3 T).

2. RESULTS

2.1. Characterization of the cobalt nanoparticles by transmission electron microscopy

Two samples (A and B) containing monodispersed water-soluble cobalt nanoparticles were synthesized. The cobalt nanoparticles were coated with alkyl thioether end-functionalized poly-(methacrylic acid) (PMAA-DDT) polymer, which makes them water-soluble. The particle size was controlled by altering the molecular weight and concentration of the polymer ligands. In sample A, a polymer with higher molecular weight was used compared with that of sample B. The mean average cobalt core diameter, measured using transmission electron microscopy (TEM), was 3.9 nm (A) and 3.3 nm (B), as shown in Fig. 1. The hydrodynamic total diameter (cobalt core + polymer coating) of the particles, measured using a dynamic light scattering technique, was 28 nm (A) and 13 nm (B), indicating a much thicker polymer coating for sample A. The cobalt cores of the two samples were therefore similar in diameter but the polymer coating was thicker for sample A.

* *Correspondence to: L. M. Parkes, Magnetic Resonance and Image Analysis Research Centre (MARIARC), The University of Liverpool, Liverpool, L69 3GE, UK. E-mail: laupar@liverpool.ac.uk*

a *L. M. Parkes, R. Hodgson*
Magnetic Resonance and Image Analysis Research Centre (MARIARC), University of Liverpool, Liverpool L69 3GE, UK

b *L. Lu, I. Robinson, N. T. K. Thanh*
Department of Chemistry, University of Liverpool, Crown Street, Liverpool, L69 7ZB, UK

c *L. Tung*
Department of Physics, University of Liverpool, Liverpool L69 7ZE, UK

d *D. G. Fernig, N. T. K. Thanh*
School of Biological Sciences, University of Liverpool, Crown Street, Liverpool, L69 7ZB, UK

e *D. G. Fernig, N. T. K. Thanh*
Liverpool Institute for Nanoscale Science, Engineering and Technology (LINSET), University of Liverpool, Crown Street, Liverpool L69 7ZB, UK

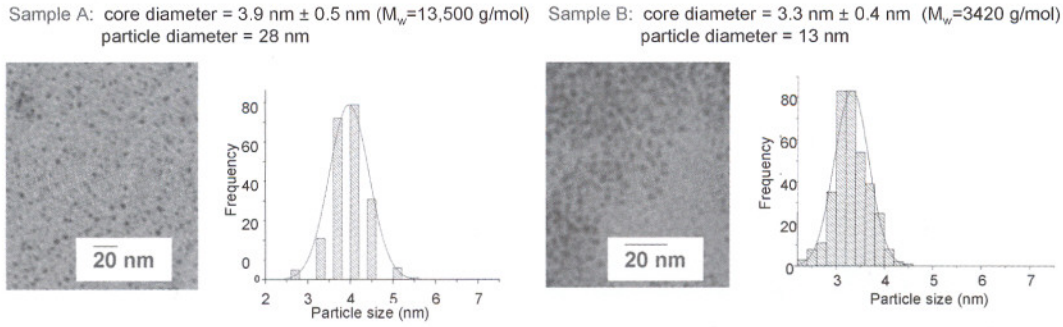

Figure 1. TEM images of the cobalt nanoparticles and the histograms. TEM images of the cobalt nanoparticles and the corresponding histograms showing the average particle size of the cobalt core in samples A (left panel) and B (right panel). The total particle diameter including the cobalt core and the polymer coating was determined by dynamic light scattering technique and its value is also given. This figure is available in colour online at www.interscience.wiley.com/journal/cmmi

2.2. DC magnetometry

The samples were magnetically characterized by means of a commercial super conducting quantum interference device (SQUID) magnetometer. Results of the zero-field-cooled (ZFC) and field-cooled (FC) magnetization measurements [Fig. 2(a)] show that the cobalt nanoparticles in both samples were superparamagnetic at 300 K. The blocking temperature (T_B), as determined from the peak of the ZFC curve, of the sample A is of about 77 K, which is slightly higher than that of about 73 K for sample B. The temperature dependence of the magnetization was also measured at a magnetic field of 5 T [Fig. 2(b)]. Because the magnetic field here is sufficiently strong, the magnetization measured at 5 T could also be considered as the saturation magnetization M_s of the sample, in particular at the temperatures below the blocking temperature T_B. At 5 K, this value is 1169 emu/cm^3 for sample A and 1125 emu/cm^3 for sample B; whilst at 300 K it becomes 806 emu/cm^3 for sample A and 700 emu/cm^3 for sample B. These values were obtained at room temperature; however extrapolation to human body temperature (310 K) has little effect of the specific magnetization (797 and 691 emu/cm^3 for A and B, respectively).

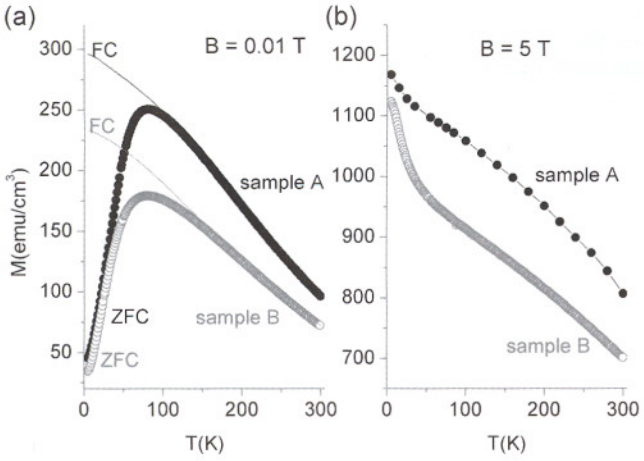

Figure 2. Magnetic properties of the cobalt nanoparticles. Zero-field-cooled (ZFC) and field-cooled (FC) magnetization as a function of temperature measured in a magnetic field of 0.01 T (a) and the magnetization as a function of temperature measured in a magnetic field of 5 T (b). This figure is available in colour online at www.interscience.wiley.com/journal/cmmi

2.3. Relaxivity measurements

The cobalt nanoparticles were dispersed in tubes of 2% agarose gel at different concentrations from 0 to 0.5 mM (i.e. millimoles of cobalt atoms per litre of agarose gel). The tubes were placed in a water bath at 40°C. Images were repeatedly collected on a Siemens 3 T Trio system in order to produce maps of the relaxation times T_1 and T_2 as the tubes cooled. The temperature was monitored by a thermometer placed in a 'dummy' tube of agarose gel. Mapping was performed at temperatures of 40, 38.5 and 37°C. The water bath and tubes were then removed from the scanner and cold water was added until the temperature was maintained at 25°C and scanning was repeated. At 1.5 T, mapping was performed at 25°C only. In order to determine whether there was any effect from possible particle aggregation during dispersion in agarose gel, measurements from nanoparticles dispersed in water were also taken. Nanoparticles were dispersed in water at concentrations from 0 to 0.8 mM, the tubes were placed in a water bath at 25°C and T_1 and T_2 mapping was performed at 1.5 T.

The same imaging parameters were used at both 3 and 1.5 T, as described in the experimental section. A multi-echo spin echo sequence was used for T_2 measurements and an inversion recovery turbo spin echo sequence for T_1 measurements. Matlab software was used to fit the signal intensity of the images on a voxel by voxel basis to the appropriate mono-exponential model in order to produce maps of T_1 and T_2. A region of interest was identified in the centre of each tube and the mean and standard deviation over voxels of the relaxation rates were recorded for each concentration. A linear fit of relaxation against concentration gave the relaxivity values r_1 and r_2 in units of mM^{-1} s^{-1}.

2.4. Effect of particle size

There was a significant difference in r_1 between samples A and B at both 3 T (Fig. 3, Table 1) and at 1.5 T (Fig. 7, Table 2). Sample A, with the larger particles, showed approximately double the value of r_1 (4.3 mM^{-1} s^{-1} at 3 T) compared with sample B (2.2 mM^{-1} s^{-1} at 3 T). At both field strengths, r_2 was greater for sample A compared with sample B, but this was only significant at 1.5 T. The high values of r_2 allow both samples to be suitable as negative contrast agents [Fig. 4(a)].

2.5. Effect of temperature

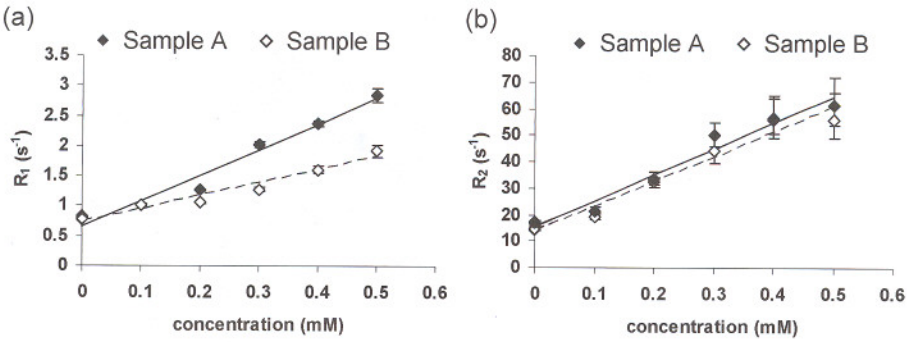

Figure 3. Effect of particle size. Relaxation rates R_1 (a) and R_2 (b) for different concentrations of the cobalt nanoparticles in samples A and B at 3 T and 37°C. Linear fits are shown, from which the relaxivities r_1 and r_2 are calculated as the gradient. The error bars represent the standard deviation of relaxation rates over the voxels in the region.

No statistically significant effect of temperature was seen on the relaxivity values (Fig. 5, Table 1), except for a trend to increase r_1 slightly with increasing temperature.

2.6. Effect of magnetic field strength

Figure 6 and Table 1 show the effect of magnetic field strength on the relaxivities. The relaxivity r_1 at 1.5 T ($7.4\ mM^{-1}\ s^{-1}$) was approximately double that at 3 T ($3.9\ mM^{-1}\ s^{-1}$). An opposite effect was seen on r_2, however, with a statistically insignificant reduction in r_2 at the lower field of 1.5 T.

2.7. Dispersion in water compared to agarose gel

Figure 7 and Table 2 show the relaxivities when the particles are dispersed in water compared with agarose gel. The absolute relaxation rates are seen to be different (Fig. 7) due to the different MR properties of water and agarose. On the other hand, the relaxivities r_1 and r_2 (Table 2) are not significantly different.

3. DISCUSSION

We have successfully synthesized cobalt nanoparticles of core size less than 4 nm and total particle size (core + coating) of 28 and 13 nm for samples A and B, respectively. The values of 'saturation' magnetization of 1169 and 1125 emu/cm^3 (for samples A and B, respectively, at 5 K) are less than the bulk value for cobalt [~1440 emu/cm^3 at 0 K (3)]. This reduction in the 'saturation' magnetization as compared with the bulk is quite common for the magnetic nanoparticles which can be attributed either to the presence of a minority of very small superparamagnetic nanoparticles at low temperature or the 'dead magnetic layer' on the surface of the particles.

On the other hand, at 300 K and 5 T, the values of the magnetization are just 806 emu/cm^3 for sample A and 700 emu/cm^3 for sample B. Since both samples are superparamagnetic at 300 K, the 5 T field is clearly not sufficient to saturate the magnetization, and thus its value is significantly lower than the saturation magnetization bulk value for cobalt [1422 emu/cm^3 at 300 K (3)]. Nevertheless, these values obtained for the cobalt nanoparticles are still much higher than the saturation magnetization of bulk iron oxide of 395 emu/cm^3 at 300 K (4). Compared with iron oxide nanoparticles, one study reported the value of the magnetization of 234 emu/cm^3 (45 emu/g) at 300 K for particles <10 nm (5). In another study, at 300 K, it was reported as 250 emu/cm^3 (48 emu/g) and 296 emu/cm^3 (57 emu/g) for 4.5 and 8.5 nm nanoparticles, respectively (6). These values reported for the iron oxides are much lower than the values found in our cobalt nanoparticles which also have smaller size of 3.9 and 3.3 nm. For small particles, relaxivity is proportional to the square of the magnetization per unit volume. Our data on the values of the magnetization thus clearly indicate the advantage of using

Table 1. Relaxivity values

	Sample				
	B	A	A	A	A
Temperature (°C)	37	37	40	25	25
Field strength (T)	3	3	3	3	1.5
r_1 ($mM^{-1}\ s^{-1}$)	$2.2 \pm 0.7^*$	$4.3 \pm 1.1^*$	4.2 ± 1.1	$3.9^\dagger \pm 1.0$	$7.4^\dagger \pm 2.0$
r_2 ($mM^{-1}\ s^{-1}$)	94 ± 26	99 ± 36	98 ± 27	105 ± 35	88 ± 32
r_2/r_1	43	23	23	27	12

Relaxivity values are given as the mean and the 95% confidence interval on the fit.
*These values are significantly different from each other ($p < 0.01$).
†These values are significantly different from each other ($p < 0.01$).

Table 2. Relaxivity values for particles dispersed in water or agarose gel

	Sample			
	A	A	B	B
Solvent	Agarose	Water	Agarose	Water
r_1 ($mM^{-1}s^{-1}$)	$7.4 \pm 2.0^*$	$6.4 \pm 1.8^\dagger$	$3.9 \pm 0.8^*$	$3.8 \pm 0.4^\dagger$
r_2 ($mM^{-1}s^{-1}$)	88 ± 32	$71 \pm 24^\ddagger$	63 ± 39	$44 \pm 5^\ddagger$

Relaxivity values measured at 25°C and 1.5 T given as the mean ± 95% confidence interval on the fit. No significant differences were found between the relaxivities in agarose gel and water.
*These values are significantly different from each other ($p < 0.01$).
†, ‡ These values are significantly different from each other ($p < 0.05$).

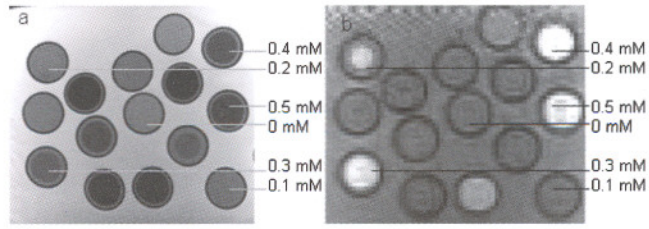

Figure 4. MR contrast at different concentrations of cobalt nanoparticles. (a) Images from a T_2-weighted spin echo sequence with an echo time of 30 ms and a repetition time of 2500 ms and (b) images from a T_1-weighted three-dimensional gradient echo sequence with repetition time of 70 ms, flip angle of 30° and an echo time of 10 ms. Darkening with increasing concentration of the cobalt nanoparticles on the T_2-weighted image (a) and brightening on the T_1-weighted image (b) demonstrates possible application as both a negative and a positive contrast agent. The concentrations for sample A are labelled.

cobalt nanoparticles over iron oxide in order to enhance the MR relaxivity.

3.1. Effect of particle size

At magnetic field strengths of 1.5 and 3 T, the relaxivity r_2 is known to increase with the square of the core diameter, as shown both theoretically for superparamagnetic particles in general (7) and experimentally for iron oxide (8). We observed r_2 relaxivity to be larger for sample A than sample B (Fig. 3, Table 1 and Fig. 7, Table 2). This is consistent with both the size and magnetization measurements of the two samples. At 300 K, sample A has saturation magnetization of 806 emu/cm^3 and size of 3.9 nm, whereas sample B has lower saturation magnetization of 700 emu/cm^3 and a smaller size of 3.3 nm. This leads to a prediction of an increase in r_2 of approximately 85% for sample A compared with sample B (proportional to the square of the magnetization and the square of the core diameter). In fact, we observed differences in r_2 of ~40% in agarose gel and ~61% in water) at 1.5 T (Fig. 7, Table 2). This discrepancy between the observed and expected values may be due to the thicker coating of sample A which would reduce the r_2 relaxivity.

The behaviour of r_1 is complex and depends not only on the particle core size and magnetic field (7,8) but also on the effect of the size and composition of the hydrophilic polymer coating on diffusion (9). A thicker coating may also improve the stability of the particle core. Optimization of the coating may therefore further increase r_1.

3.2. Effect of temperature

Although there was a trend to increase r_1 slightly with increasing temperature, we find almost no change in r_2 relaxivity with temperature. For r_1, the results are consistent with water diffusion limiting T_1 relaxivity and the cobalt nanoparticles become more accessible to water molecules at higher temperatures, as the diffusion coefficient increases. The results for the cobalt nanoparticles contrast with those for Gd-DTPA, which shows a relatively large decrease in r_1 with increasing temperature—about 30% over a similar temperature range (10). The temperature independence of the relaxivities for the cobalt nanoparticles may be of benefit for *in vivo* scanning where temperatures may vary slightly between body sites and subjects.

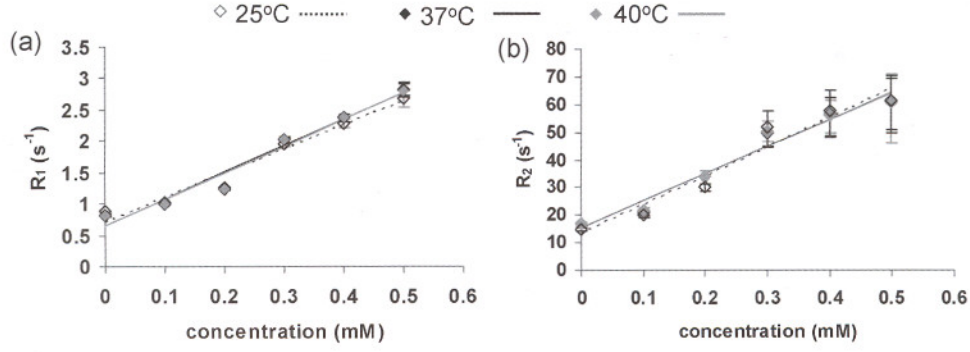

Figure 5. Effect of temperature. Relaxation rates R_1 (a) and R_2 (b) for different concentrations of the cobalt nanoparticles in sample A at 3 T at different temperatures. Linear fits related to the relaxivities are shown. The error bars represent the standard deviation of relaxation rates over the voxels in the region. This figure is available in colour online at www.interscience.wiley.com/journal/cmmi

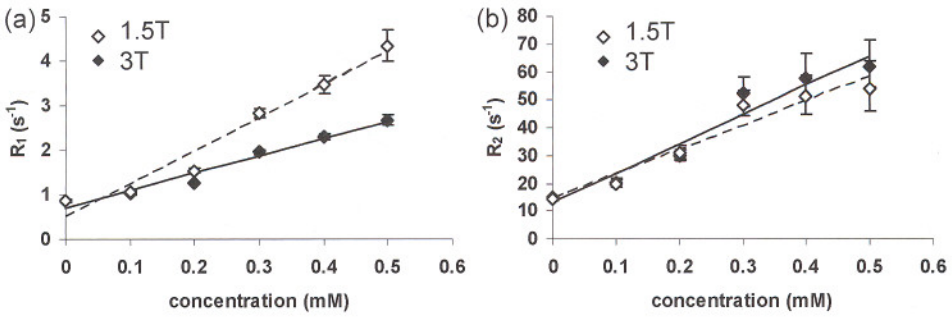

Figure 6. Effect of magnetic field strength. Relaxation rates R_1 (a) and R_2 (b) for different concentrations of the cobalt nanoparticles in sample A at the magnetic field strengths of 1.5 and 3 T at 25°C. Linear fits related to the relaxivities are shown. The error bars represent the standard deviation of relaxation rates over the voxels in the region.

3.3. Effect of magnetic field strength

The decrease in r_1 with increasing magnetic field strength is in accordance with the theory of Roch and Muller (7). This, and the opposite effect on r_2 is supported by empirical evidence from a study of USPIOs (11).

3.4. Dispersion in water compared with agarose gel

We find that r_1 and r_2 are similar whether the cobalt nanoparticles are dispersed in water or agarose gel, suggesting that there is no further aggregation of particles on dispersion in agarose gel.

3.5. Relaxivity values

The highest relaxivities were obtained at 1.5 T with values for r_1 and r_2 of 7.4 and 88 $mM^{-1}s^{-1}$, respectively. These values are smaller than those for the USPIO Ferumoxtran-10 in free solution (marketed as Sinerem, Guebert group or Combidex, Advanced Magnetics), which were reported to be 15.5 and 100 $mM^{-1}s^{-1}$ for r_1 and r_2, respectively at 1.5 T (11). A recent comprehensive report compared r_1 and r_2 values of 14 commercially available contrast agents including gadolinium and iron oxide agents (12). The gadolinium agents all had similar relaxivities, such as Gd-DTPA with r_1 and r_2 of 3.3 and 3.9 $mM^{-1}s^{-1}$, respectively, in water at 1.5 T and 37°C. The two commercially available iron oxide agents tested had r_1 and r_2 values of 8.7 and 61 $mM^{-1}s^{-1}$ (Resovist) and 4.7 and 41 $mM^{-1}s^{-1}$ (Feridex/Endorem). The relaxivities reported for the cobalt nanoparticles are similar to those from the iron oxide agents. Measurements of the iron oxide core diameters range from 4.3 to 9.5 nm (13,14), i.e. larger than the cobalt core diameter in our study. Interestingly, a recent study using FeCo nanoparticles with similar core sizes of 4 nm reported larger r_1

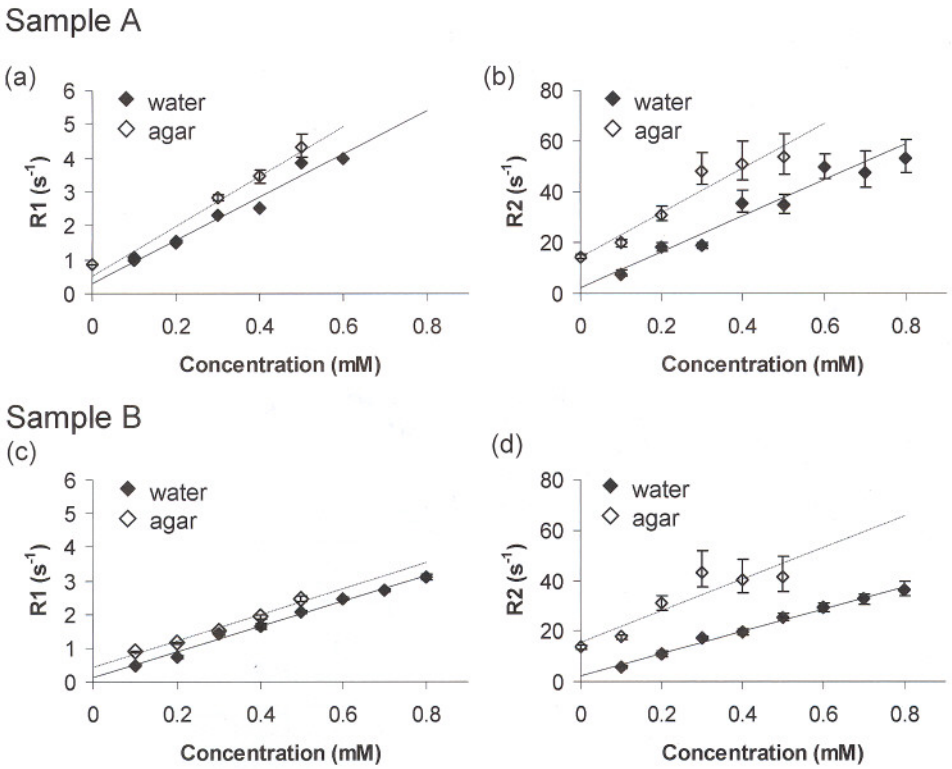

Figure 7. Dispersion in water compared to agarose gel. Relaxation rates R_1 (a, c) and R_2 (b, d) for different concentrations of cobalt nanoparticles in sample A (a and b) and sample B (c and d) in both water (solid symbols) and agarose gel (open symbols) at 1.5 T and 25°C. Linear fits related to the relaxivities are shown. The error bars represent the standard deviation of relaxation rates over the voxels in the region.

and r_2 relaxivities at 1.5 T of 31 and 185 $mM^{-1}s^{-1}$, respectively (15), supporting the advantage of using transition metals. These relaxitivites of the FeCo nanoparticles were higher than those reported here for cobalt nanoparticles. This may be due to the ultra-thin single-graphitic shell structure of the core in the FeCo nanoparticles and differences in coating.

Assuming a mono-exponential decay curve to estimate T_2 and T_1 is only an approximate model of the true condition, but this is unlikely to have a large effect on the calculated values of the relaxivities. For example, for the worst case of the longest T_1 (1200 ms for pure agarose gel) and the repetition time (TR) of 5850 ms, including the additional term $[\exp(-TR/T_1)]$ in the T_1 model (16) gives less than a 2% increase in the estimated value of T_1.

3.6. Toxicity of cobalt nanoparticles

The toxicity effects of cobalt in man are difficult to evaluate, as they are also dependent on nutritional factors (17). Many patients have taken up to 50 mg cobalt/day as Roncovite® for refractory anemia for long periods with little or no toxicity. Roncovite® also contains 100 mg of ferrous sulfate, which may have affected the amount of cobalt absorbed, since cobalt and iron share a common absorption pathway. In contrast, 10 mg cobalt/day taken by heavy beer drinkers in the 1960s may have resulted in cardiomyopathy (17), as the effect of inadequate protein intake, thiamine intake, zinc depletion and alcohol may render the heart more sensitive to Co^{2+} toxicity. There are currently no data on the toxicity of cobalt in the form of nanoparticles. It is important to note that, by keeping the cobalt nanoparticles stable from chemical oxidation through the design of appropriate ligand shells, it will not only retain the magnetization of the nanoparticles, but also prevent the formation of Co^{2+}, which can be released into solution and is potentially toxic. Thus, stable nanoparticles will be seen by the body as the ligand shell, not the underlying cobalt metal, and are likely not to be toxic; excretion will in this case be of the entire nanoparticles. Consequently, there may well be the potential for cobalt to be used in humans after suitable toxicity and pharmacokinetic studies in animals.

4. CONCLUSION

The r_1 and r_2 relaxivities of cobalt nanoparticles have been measured at a range of temperatures and two magnetic field strengths. The high value for r_2 shows that the cobalt nanoparticles have potential as a negative contrast agent. The nature of the polymer coating appears to have a large effect on r_1. The relaxivity values for the cobalt nanoparticles are similar to those reported for iron oxide with larger core size, suggesting that the cobalt nanoparticles have potential as an alternative contrast agent to iron oxide.

5. EXPERIMENTAL

5.1. Particle synthesis and characterization

Monodispersed water-soluble cobalt nanoparticles were prepared by the reduction of cobalt salt in aqueous solution in the presence of alkyl thioether end-functionalized PMAA-DDT ligands (18). The size of the cobalt particles was controlled by varying the molecular weight and concentration of the polymer. For synthesis of the cobalt nanoparticles in sample A and B, 0.12 mM of the polymer with molecular weight $M_w = 13\,500$ g/mol and 0.06 mM of the polymer with molecular weight $M_w = 3{,}420$ g/mol were used, respectively.

The morphology including the size and shape of the nanoparticles was examined by TEM. In TEM, 5 μl of the diluted sample were dropped on a carbon-coated copper TEM grid at room temperature and left to evaporate slowly in air. Images were obtained using a FEI Tecnai G^2 120 kV TEM, operated at 100 kV and visualized using analySIS software. The average core diameter of the nanoparticles containing only cobalt was taken as the mean of a minimum of 200 nanoparticles measured from enlarged photographs using Bersoft Image Measurement 1.0 software. The hydrodynamic diameters (cobalt core + polymer coating) of the particles were measured using a dynamic light scattering technique with Zetanano S (Zen 3600), Malvern Instruments Inc.

The magnetic properties of the samples were investigated in the super conducting quantum interference device (SQUID) magnetometer in the temperature range 5–300 K and magnetic field up to 5 T.

5.2. MRI scanning parameters

The same imaging parameters were used at both 3 T (Siemens Trio) and 1.5 T (Siemens Symphony). The body coil was used for radio frequency transmission and an eight-channel phased-array head coil for signal collection.

5.2.1. T_2 quantification

A multi-echo spin echo sequence was used with the following parameters: 16 echo times from 15 to 240 ms, repetition time of 2.5 s, band-width of 130 Hz/pixel, in-plane resolution of 0.9 × 0.9 mm, seven slices of 5 mm thickness with 5 mm gap and scanning time of 5 min.

5.2.2. T_1 quantification

An inversion recovery turbo spin echo sequence was used with the following parameters: echo time of 6.2 ms, repetition time of 5.85 s, bandwidth of 501 Hz/pixel, turbo factor of 3, in-plane resolution of 0.9 × 1.4 mm and 20 slices of 3 mm thickness with 1 mm gap. Scanning time was 4 min and was repeated five times with inversion times of 100, 570, 750, 1500 and 3000 ms in a random order. At 1.5 T the bandwidth was increased to 574 Hz/pixel.

5.3. Analysis

Matlab was used to fit the signal intensity of the images on a voxel by voxel basis to the appropriate mono-exponential model:

$$S = S_0 e^{-TE/T_2} \qquad \text{for } T_2 \tag{1}$$

$$S = S_0(1 - 2e^{-TI/T_1}) \qquad \text{for } T_1 \tag{2}$$

Least squares minimization was used to perform two-parameter fits for S_0 and the relaxation constant, producing maps of T_1 and T_2. When fitting for T_2, only seven data points from echo times of 15–90 ms were used, as the signal had largely decayed away for echo times greater than this, introducing only noise into the data. A region of interest was identified in the centre of each tube, containing at least 50 voxels (approximately 200 mm^3). The mean and standard deviation over voxels of the relaxation rates (i.e. R_1 and R_2, the reciprocal of the relaxation times T_1 and T_2) were recorded for each concentration to produce

plots of relaxation rate vs concentration. A linear fit gave the relaxivity values for r_1 and r_2 in units of $mM^{-1}s^{-1}$. The 95% confidence interval on the relaxivity values was calculated by multiplying the standard error of the fitted slope by 2.78 (for 6 degrees of freedom).

Acknowledgements

This work was funded by the North West Cancer Research Fund, the Engineering and Physical Sciences Research Council (EP/C511794/1) the Wellcome Trust, the Vietnamese Government (322 project), and a University of Liverpool Interdisciplinary Research Award. Richard Hodgson is funded by a Research Fellowship from Royal College of Radiologists, UK and Nguyen TK Thanh a Royal Society University Research Fellowship.

REFERENCES

1. Pankhurst QA, Connolly J, Jones SK, Dobson J. Applications of magnetic nanoparticles in biomedicine. J. Phys. D. Appl. Phys. 2003; 36(13): R167–R181.
2. Kim DK, Zhang Y, Voit W, Kao KV, Kehr J, Bjelke B, Muhammed M. Superparamagnetic iron oxide nanoparticles for bio-medical applications. Scripta Mater. 2001; 44(8–9): 1713–1717.
3. Lide DR. Handbook of Chemistry and Physics. CRC Press: Boca Raton, 1992.
4. Clark DJ. Magnetic Oxides. Wiley: New York, 1972; 689.
5. Bautista MC, Bomati-Miguel O, Zhao X, Morales MP, Gonzalez-Carreno T, de Alejo RP, Ruiz-Cabello J, Veintemillas-Verdaguer S. Comparative study of ferrofluids based on dextran-coated iron oxide and metal nanoparticles for contrast agents in magnetic resonance imaging. Nanotechnology 2004; 15(4): S154–S159.
6. Li Z, Tan B, Allix M, Cooper AI, Rosseinsky MJ. Direct coprecipitation route to monodisperse dual-functionalized magnetic iron oxide nanocrystals without size selection. Small 2008; 4(2): 231–239.
7. Roch A, Muller RN, Gillis P. Theory of proton relaxation induced by superparamagnetic particles. J. Chem. Phys. 1999; 110(11): 5403–5411.
8. Allkemper T, Bremer C, Matuszewski L, Ebert W, Reimer P. Contrast-enhanced blood-pool MR angiography with optimized iron oxides: effect of size and dose on vascular contrast enhancement in rabbits. Radiology 2002; 223(2): 432–438.
9. Paul KG, Frigo TB, Groman JY, Groman EV. Synthesis of ultrasmall superparamagnetic iron oxides using reduced polysaccharides. Bioconjug. Chem. 2004; 15(2): 394–401.
10. Strijkers GJ, Mulder WJM, van Heeswijk RB, Frederik PM, Bomans P, Magusin P, Nicolay K. Relaxivity of liposomal paramagnetic MRI contrast agents. Magn. Reson. Mater. Phys. Biol. Med. 2005; 18(4): 186–192.
11. Simon GH, Bauer J, Saborovski O, Fu YJ, Corot C, Wendland MF, Daldrup-Link HE. T_1 and T_2 relaxivity of intracellular and extracellular USPIO at 1.5 T and 3 T clinical MR scanning. Eur. Radiol. 2006; 16(3): 738–745.
12. Rohrer M, Bauer H, Mintorovitch J, Requardt M, Weinmann HJ. Comparison of magnetic properties of MRI contrast media solutions at different magnetic field strengths. Invest. Radiol. 2005; 40(11): 715–724.
13. Jung CW, Jacobs P. Physical and chemical-properties of superparamagnetic iron-oxide mr contrast agents—ferumoxides, ferumoxtran, ferumoxsil. Magn. Reson. Imag. 1995; 13(5): 661–674.
14. Li W, Tutton S, Vu AT, Pierchala L, Li BSY, Lewis JM, Prasad PV, Edelman RR. First-pass contrast-enhanced magnetic resonance angiography in humans using ferumoxytol, a novel ultrasmall superparamagnetic iron oxide (USPIO)-based blood pool agent. J. Magn. Reson. Imag. 2005; 21(1): 46–52.
15. Seo WS, Lee JH, Sun XM, Suzuki Y, Mann D, Liu Z, Terashima M, Yang PC, McConnell MV, Nishimura DG, Dai HJ. FeCo/graphitic-shell nanocrystals as advanced magnetic-resonance-imaging and near-infrared agents. Nature Mater. 2006; 5(12): 971–976.
16. Gowland PA, Stevenson VL. T_1: the longitudinal relaxation time. In: Quantitative MRI of the Brain, Tofts PS (ed). Wiley: Chichester, 2003; 111–142.
17. Alexander CS. Cobalt–Beer cardiomyopathy–clinical and pathologic study of 28 cases. Am. J. Med. 1972; 53(4): 395–417.
18. Robinson I, Alexander C, Lu LT, Tung LD, Fernig DG, Thanh NTK. One-step synthesis of monodisperse water-soluble 'dual-responsive' magnetic nanoparticles. Chem. Commun. 2007; 44: 4602–4604.